Available online at www.sciencedirect.com
ScienceDirect
Ceramics International 37 (2011) 1825–1831
CERAMICS INTERNATIONAL
www.elsevier.com/locate/ceramint

Hydroxyapatite extracted from fish scale: Effects on MG63 osteoblast-like cells

Yi-Cheng Huang [a,*], Pei-Chi Hsiao [a], Huey-Jine Chai [b]

[a] College of Life Sciences, Department of Food Science, National Taiwan Ocean University, No. 2, Pei-Ning Road, Keelung 20224, Taiwan
[b] Seafood Technology Division, Fisheries Research Institute, Council of Agriculture, Keelung 20246, Taiwan

Received 4 January 2011; received in revised form 28 January 2011; accepted 31 January 2011
Available online 5 March 2011

Abstract

In recent years, environmental and economic conditions have raised concerns about the treatment and use of bio-waste. This study analyzed hydroxyapatite extracted from fish scale (FHAP) by enzymatic hydrolysis. The structures of FHAP were characterized by Fourier transform infrared spectroscopy, particle size analyzer, scanning electron microscopy, X-ray diffraction, and energy dispersive spectrometry. The analytical results indicated that FHAP consisted of nano-sized particles with Ca/P ratio of 1.76. After FHAP particles were sintered at 800°C for 4 h, the particles showed increased porosity and surface roughness. The influence of FHAP particles on the proliferation and osteogenic differentiation of MG63 cells was also investigated. Compared with hydroxyapatite from Sigma (SHAP), FHAP significantly increased MG63 growth, whether hydroxyapatite powders were sintered or not. Under osteogenic-inductive culture condition, FHAP particles promoted osteogenic differentiation and mineralization of MG63 cells, which was confirmed by alkaline phosphate assay and von Kossa staining. This study confirms that FHAP extracted by enzymatic hydrolysis is a promising biomaterial for artificial bone fabrication.

Keywords: A. Sintering; Hydroxyapatite; Fish scale; Bio-waste; Enzymatic hydrolysis

1. Introduction

Each year, 18–30 million tons of fish waste is discarded throughout the world [1]. Fish waste is a potential source of protein of high biological value, unsaturated essential fatty acids, vitamins and antioxidants, minerals or trace metals, and physiological beneficial amino acids and peptides [2]. Therefore, fish waste has tremendous unexploited potential for adding value. However, the use of fish waste in foods and biochemical products for human consumption is still under intensive study in the aquaculture industry. The fish waste examined in this study was fish scale.

By weight, about 50% of the total waste generated by the fish processing industry is waste, and about 4% of the waste is fish scale. Generally, fish scale is considered worthless, impracticable, and dismissed as a waste. However, it is known that fish scale contains numerous valuable organic and inorganic components, mainly collagen and hydroxyapatite [3], which have commercial value for use in manufacturing functional foods, cosmetics, and biomedical products [4–6].

Collagen is the most abundant animal protein and has numerous biomedical and pharmaceutical applications. Therefore, most studies of fish scale waste have focused on isolating and characterizing collagen [5,7–9]. In recent years, hydroxyapatite has attracted interest for use in bone grafting because of their osteoconductive and bioactive properties [10,11]. Other medical applications of hydroxyapatite have also been studied because hydroxyapatite is biocompatible, bioactive, non-toxic, non-inflammatory and non-immunogenic [12,13]. Natural hydroxyapatite bioceramics have recently been extracted from various bio-waste, including corals [14,15], cuttlefish shells [16], porcine teeth and bones, and bovine bones [12,13]. Chemical analysis shows that these products, which would otherwise be considered bio-waste, are rich sources of calcium. Compared with hydroxyapatite produced by synthetic methods such as expeditious microwave irradiation [17], chemical precipitation [18] and radio frequency thermal plasma [19], extraction of hydroxyapatite from bio-waste is a biologically

* Corresponding author. Tel.: +886 2 24622192x5119; fax: +886 2 24634203.
E-mail address: ychuang@mail.ntou.edu.tw (Y.-C. Huang).

0272-8842/$36.00
doi:10.1016/j.ceramint.2011.01.018

safe (*i.e.*, no chemicals are required) and a potentially lucrative process, especially given the growing global demand for hydroxyapatite bioceramics [13]. Therefore, the hydroxyapatite used in this work is extracted from fish scale by enzymatic hydrolysis.

The objective of this study was to characterize FHAP extracted by enzymatic hydrolysis, and evaluate the potential use of FHAP for artificial bone application. After characterizing the physical and chemical properties of FHAP, particles of FHAP were co-cultured with MG63 cells to investigate their effects on cell proliferation and osteogenic differentiation. Gaining insight into the interactions between FHAP particles and cells could provide essential information about the biological properties of FHAP and its potential use as a biomaterial for bone repair.

2. Materials and methods

Dulbecco modified Eagle medium: nutrient mixture F-12 (DMEM/F12), fetalbovine serum (FBS), 1% penicillin/streptomycin, 1% L-glutamine, 1% NEAA (non-essential amino acids) and trypsin were purchased from Gibco (Grand Island, NY). The hydroxyapatite (SHAP) was purchased from Sigma (No. 289396, St. Louis, MO). All other chemicals used in the study were of reagent grade and were also purchased from Sigma unless otherwise stated.

2.1. Extraction of hydroxyapatites from fish scales

Fish scale hydroxyapatite was isolated from tilapia (*Oreochromis* sp.) scales (Ko-Fwu Fishes Co., Taiwan) by enzymatic hydrolysis. In short, after washing to remove impurities, the fish scales were crushed with a disperser (Kinematica, NY, USA), then hydrolyzed under 1% protease N for 2.5 h, and 0.5% flavourzyme (Novozymes, Chiba-shi, Japan) for another 0.5 h at an optimal pH and temperature. Hydrolysates were stirred and heated in a boiling water bath for 10 min to deactivate enzymes. The hydrolysates were then centrifuged at 12,000 × *g* for 20 min; the residues were dried by hot air and stored at −20°C until use. Additionally, the FHAP particles were sintered at 800°C for 4 h, and SHAP was used for comparison.

2.2. Characterization of FHAP powder

The phase composition of the HAP powder was assessed by XRD (X-ray diffraction model: Panalytical X'Pert ProMPD) with the 2θ range from 20° to 60° and a step size of 0.1°. Particle size distribution and apparent density were analyzed separately with a particle size analyzer (Malvern Nano-ZS/ISO13321) and an automatic gas displacement pycnometer (Micromeritics AccuPyc1340), respectively. Energy dispersive spectrometry (EDS) was used for element analysis, and a Fourier transform infrared spectrometer (FTIR, Brucker Tensor 27) was used to characterize the compound. Both spectra were collected and analyzed using the standard software package provided by the manufacturer. The morphology of the HAP powder was viewed by scanning electron microscopy (Jeol JSM-7000F FE-SEM, Japan). The protein remaining in FHAP after sintering is analyzed by micro-Kjeldahl method [20].

2.3. Cell seeding and culture

The MG63 osteoblast-like cells (ATCC, CRL-1427) were cultured in DMEM/F12 medium supplemented with 10% fetal bovine serum, 1% penicillin/streptomycin, 1% L-glutamine, 1% NEAA (non-essential amino acids) and 1% pyruvate at 37 °C under a humidified atmosphere containing 5% carbon dioxide. The medium was changed three times a week.

2.4. Cell proliferation

After confluence of the cultures, the cells were trypsinized and added into 96-well tissue culture dishes at a density of 3×10^3 cells/well. One day later, varying concentrations of FHAP (or SHAP) suspensions (*i.e.*, 0, 5, 10, 20, and 40 μg FHAP (or SHAP) particles per milliliter of culture media) were added into each well. After co-culture for 24 h, particles were rinsed from the cells in order to analyze cell activities.

The viability of MG-63 cells was assessed by MTT (3-(4, 5-dimethylthiazol-2-yl)-2, 5-diphenyl tetrazolium bromide) assay. Absorbance was measured at 570 nm and 630 nm (SpectraMax 340PC^{384} Microplate Spectrophotometers). Cell viability was expressed as the percentage of that observed in the control specimens.

2.5. Cell differentiation

To analyze the effects of FHAP (or SHAP) particles on the osteogenic differentiation of MG-63 cells, 3×10^3 cells were added into each well of a 96-well plate. One day later, FHAPs (or SHAPs) at concentrations of 0, 5, 10, 20, and 40 μg/ml of culture media were added into each well. The FHAPs (or SHAPs) and MG-63 cells were co-cultured in osteogenic inductive media (standard culture media supplemented with 56 μg/ml ascorbic acid, 2.42 mg/ml β-glycerophosphate, and 50 μM dexamethasone). After co-culture for a specified period, particles were rinsed from the cells. The cells were subjected to alkaline phosphatase activity analysis and von Kossa staining.

2.5.1. Alkaline phosphatase activity assay

Alkaline phosphatase activity was assayed using the method described in Miyajima [21]. Briefly, after co-culturing FHAP (or SHAP) particles and MG-63 for 10 days, particles were washed twice with PBS before adding 150 μl SIGMA FAST pNPP substrate solution (Sigma, N2770), which is composed of cell lysis buffer and p-nitrophenyl phosphate. After 30 min incubation at 37°C, enzyme activity was terminated by adding 38 μl 3 M NaOH. Liberated p-nitrophenol was then measured by the light absorbance observed at 405 nm. The amount of p-nitrophenol corresponded to alkaline phosphatase activity.

2.5.2. von Kossa staining

For von Kossa staining, cells were seeded on a 24-well plate at a density of 1×10^5 cells/well. After a 3-week co-culture of FHAP (or SHAP) particles and MG-63, the cells were washed thrice with PBS then fixed with 10% formaldehyde (Sigma) for 1 h. The cells were then washed twice with distilled water and incubated with 5% silver nitrate (Sigma) for 1 h under UV illumination. After removing the silver nitrate, 5% sodium thiosulfite (Sigma) was added. The cells were then stained with Safranin T (Sigma) and observed using reverse phase-contrast microscopy.

2.6. Statistical analysis

All quantitative data were expressed as means ± S.D. Statistical analyses, including two-way ANOVA and post-test, were performed using GraphPad Prism 5. A p value of <0.05 was considered statistically significant.

3. Results and discussion

3.1. Characterization of hydroxyapatite powder

By enzymatic hydrolysis, the XRD pattern of the hydroxyapatite extracted from fish scale (FHAP) is shown in Fig. 1A. All data were collected over the 2θ range, 20° to 60° with a step size of 1°. Comparison of the brag peaks presented in the sample with the diffraction standards established by the Joint Committee on Powder Diffraction Standards for hydroxyapatite (JCPDS 00-009-0432, Fig. 1B) confirmed the composition of FHAP. Additionally, all detected FHAP peaks were broader compared to the standards.

Fig. 2A, a SEM micrograph of the as-received FHAP particles, reveals that the powder was slightly elongated. Accordingly, the broad peaks exhibited in XRD pattern (Fig. 1A), possibly due to nano-scale particles on the surface (Fig. 2B). As Fig. 2D and E shows, the hydroxyapatite from sigma (SHAP) particles presented an irregular micro-scale spherical morphology with increased surface smoothness in comparison with FHAP particles. After sintering for 4 h at 800°C, the FHAP powder became porous particles (Fig. 2C). Compared with sintered SHAP (Fig. 2F), the FHAP particles had rougher surfaces and larger surface areas. As Fig. 3A shows, experimental tests of particle size in the FHAP powders revealed a mono-modal distribution with an average size of 719.8 nm. The apparent density of the FHAP powder, which was calculated by dividing mass by average volume, was 1.8419 g/cm^3.

Fig. 3B presents the results of EDS analysis of the FHAP powders. The FHAP powders consisted of calcium (Ca), phosphorous (P), oxygen (O) and carbon (C) atoms. The analytical results indicated that the FHAP powders were rich in calcium and phosphorous in the form of carbonate and phosphate. The relative ratio of calcium to phosphorous (Ca/P) was approximately 1.78, which is slightly higher than the 1.67 ratio observed in human bones.

Fig. 3C shows the characteristic absorption peaks of FHAP powder revealed by FTIR analysis. The bands at 563, 957, and 1030 cm^{-1} indicated asymmetric bending vibrations, symmetric stretching, and asymmetric stretching of phosphate group (PO_4^{3-}), respectively. Carbonate group (CO_3^{2-}) in the FTIR spectra was identified by intense bands at 876 and 1412–1547 cm^{-1} associated with out-of-plane bending mode and asymmetric stretching, respectively. Hydroxyl group (OH^-) was identified by the small absorption band at 3670–3570 cm^{-1}, which was associated with the stretching mode of hydroxyl group. A wide absorption band observed at 3100–3500 cm^{-1} was attributed to water (H_2O), and a small band at 2365 was attributed to potassium bromide (KBr) [22]. Accordingly, the presence of the carbonate group was confirmed by both FTIR and EDS analysis.

Fig. 4 displays cell viability on FHAP and SHAP with and without sintering. According to the experimental results shown in Fig. 4A, FHAP significantly promoted the viability of MG63 cells, especially at concentrations of 10 μg/ml and 20 μg/ml. At concentrations lower than 10 μg/ml or higher than 20 μg/ml, the effect of FHAP particles on MG63 cells was not statistically significant. Moreover, the effect of FHAP particles on cell viability was superior to that of SHAP, regardless of concentration. A tentative interpretation is that the low number of peptides residing on FHAP powders contributes to cell adhesion. In addition, the differing particle size between FHAP

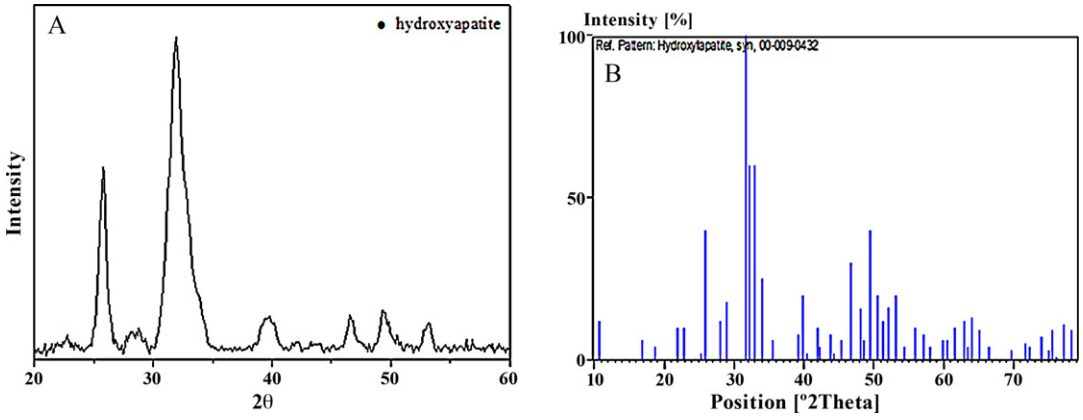

Fig. 1. X-ray diffraction pattern of (A) FHAP and (B) the stoichiometric hydroxyapatite (JCPDS 00-009-0432).

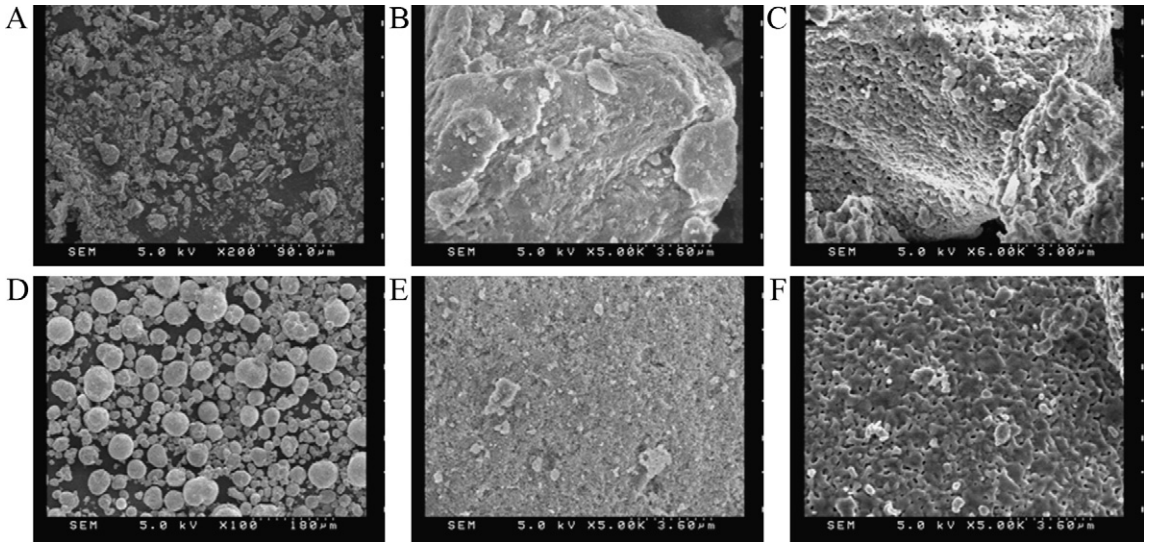

Fig. 2. SEM micrograph of the FHAP powder (A and B), sintered FHAP powder (C), SHAP powder (D and E) and sintered SHAP powder (F).

(nano-scale) and SHAP (micro-scale) may also affect cell viability [23]. Previous research [24] indicates that nano-scale particles contribute to cell viability and cell function.

To confirm the effects of peptide residences and physical properties on cell viability, sintered FHAP and sintered SHAP were co-cultured with MG63 cells. Sintered FHAP significantly promoted cell viability at concentrations of 5 μg/ml, 10 μg/ml and 20 μg/ml (Fig. 4B). At concentrations exceeding 20 μg/ml, FHAP particles clearly inhibited cell proliferation. Compared with sintered FHAP, original FHAP promoted more cell proliferation. The likely explanation for these experimental results is the amount of resident protein in FHAP. All crude proteins existing in FHAP were denatured when sintering temperature exceeding 600°C (Fig. 4D). In contrast, sintered

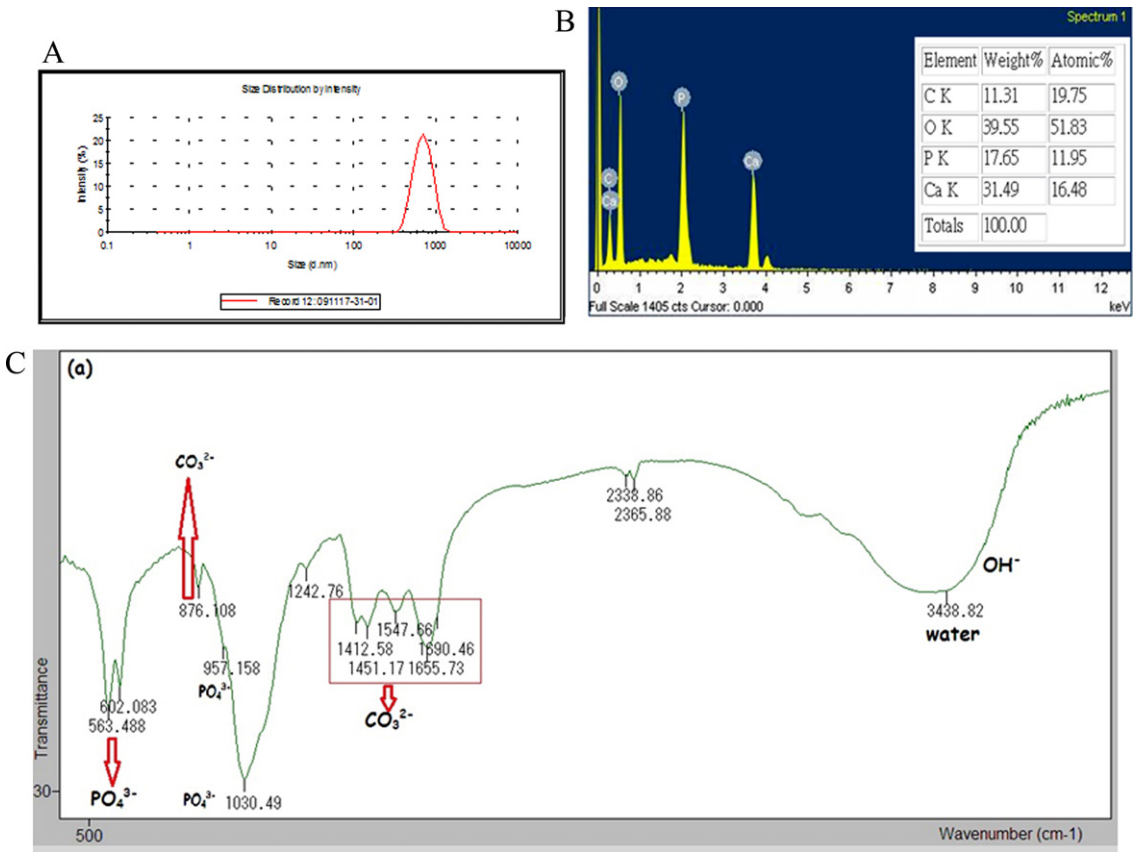

Fig. 3. Analysis of FHAP powder: (A) particle size distribution; (B) EDS analysis; (C) FTIR spectra.

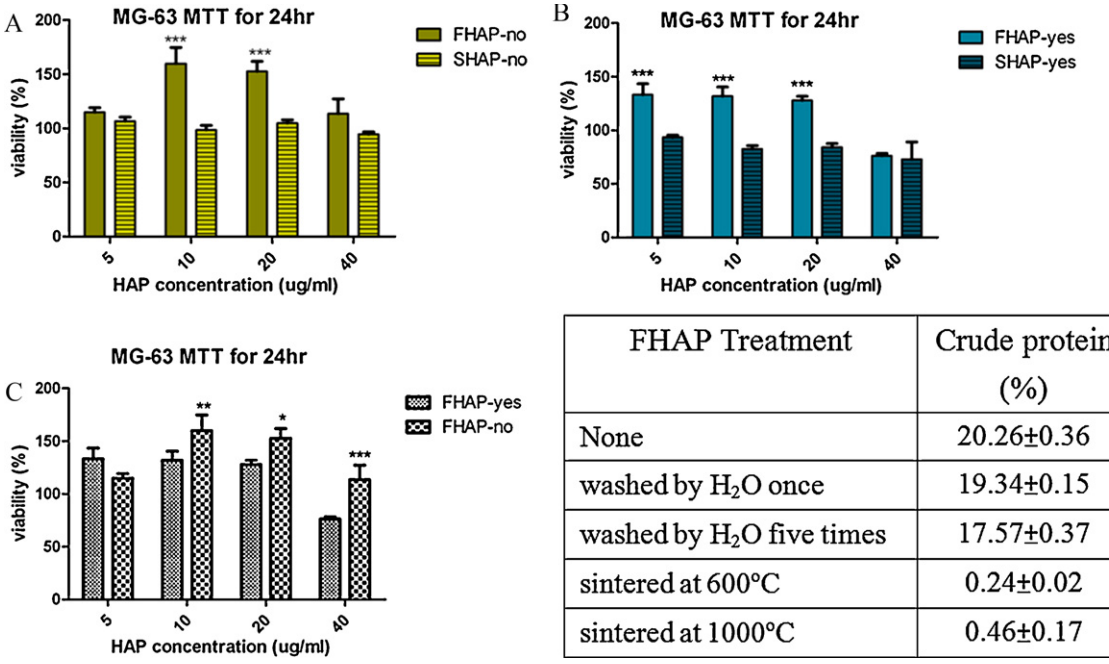

FHAP Treatment	Crude protein (%)
None	20.26±0.36
washed by H_2O once	19.34±0.15
washed by H_2O five times	17.57±0.37
sintered at 600°C	0.24±0.02
sintered at 1000°C	0.46±0.17

Fig. 4. (A–C) Effects of FHAP particles on cell viability, as assessed by a MTT method. (D) Crude protein residence with various treatments. Error bars show the standard deviation for $n = 6$. ''Yes'' means with sintered; ''no'' means without sintered.

SHAP particles revealed no obvious promoting effects on cell viability (Fig. 4B). Physical properties, including density, porosity and crystallization, are probably other key factors in cell viability [25,26]. The SEM images of sintered FHAP particles (Fig. 2) confirmed that sintering increased their density, porosity, and surface roughness. Previous studies indicate that cell adhesion correlates with substrate surface roughness [27,28]. As surface roughness increases, cell adhesion ratio increases.

Briefly, FHAP exhibited better cell viability compared to SHAP, whether or not hydroxyapatite powders were sintered. Until now, fish scales have been considered worthless. However, this study showed that FHAP is even more effective than SHAP in increasing cell viability. These results are promising because they confirm that FHAP, which until now has been considered a waste product, has potential value for use in bone repair.

A suitable osteo-induction model requires that cells be capable of differentiating into bone-forming cells. Alkaline phosphate (ALP), which is a marker of the osteoblastic phenotype, is expressed when progenitor cells differentiate into osteoblasts. Therefore, as the number of osteoblasts increase, ALP activity increases. The ALP assay is often used to evaluate cell differentiation abilities. In this study, the FHAP and SHAP particles did not significantly differ in promoting cell differentiation, regardless of whether they were sintered (Fig. 5). However, at concentrations of 40 μg/ml and 10 μg/ml (Fig. 5A and B, respectively), significant differences were noted between FHAP and SHAP. These outcomes indicate that FHAP positively affects MG-63 cell differentiation; moreover, its effect is larger than that of SHAP. Additionally, the changes in the physical properties of hydroxyapatite particles caused by the sintering process did not significantly affect the differentiation abilities of MG-63 cells.

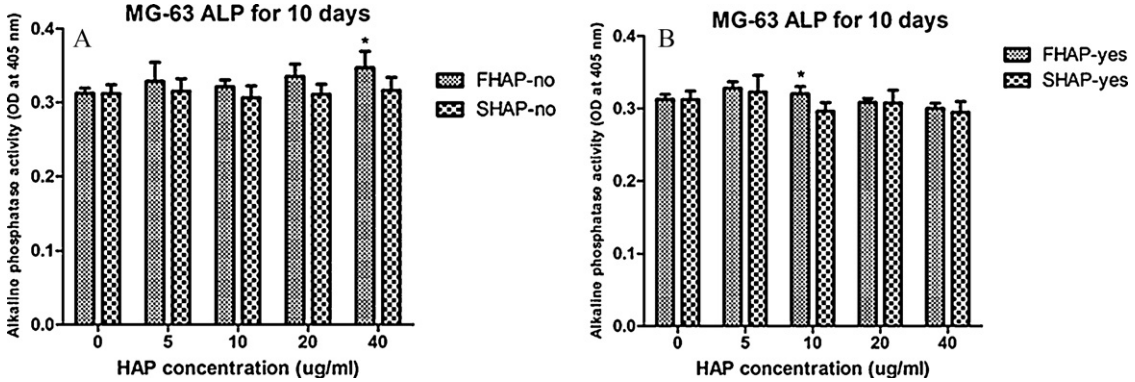

Fig. 5. The alkaline phosphatase activity of MG63 cells on FHAP and SHAP particles after culturing for up to 10 days. ''Yes'' means sintered; ''no'' means without sintered. Error bars show the standard deviation for $n = 6$.

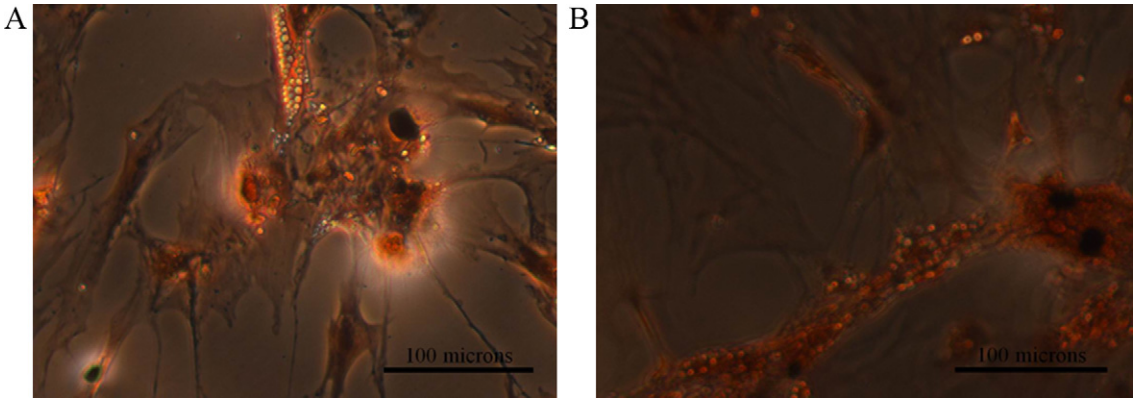

Fig. 6. von Kossa stains of MG63 cells cocultured with (A) 20 μg/ml FHAP particles and (B) 20 μg/ml SHAP particles.

Evaluating mineralized module formation is an effective method of assessing bone development. Previous studies indicate that the properties of mineralized modules, including morphologies, ultra-structures and biochemical characteristics, are similar to those of embryonic/woven bone [29–31]. The development of mineralized modules and *in vivo* bone formation are very similar. Thus, a common *in vitro* method of examining mineralization in cell cultures or in cell/biomaterial constructs is von Kossa staining. Mineralized matrix formation is the most reliable indicator of the osteoinductive capacity of materials. The experimental results in Fig. 6 show that significant mineralization occurred in both FHAP- and SHAP-treated cells. Moreover, the pseudopodium of FHAP-treated cells was more extensive compared to that of SHAP-treated cells. As indicated by the *in vitro* mineralization, MG-63 cells can differentiate into bone forming cells.

4. Conclusions

The aim of this study was to extract a bio-waste hydroxyapatite from fish scale (FHAP) using enzymatic hydrolysis and evaluate its potential use as a biomaterial. This study compared the composition and biological properties of FHAP with those of hydroxyapatite purchased from Sigma (SHAP). The experimental results showed that the FHAP were nano-sized particles with high Ca/P ratio. Compared with SHAP, the sintering process increased porosity and surface roughness in FHAP. The MTT test, ALP activity, and von Kossa staining confirmed that the FHAP promote cell proliferation and differentiation. Therefore, FHAP has potential medical applications, and fish scales provide a cost-effective, and environmentally friendly source of hydroyxapatite.

Acknowledgments

The authors would like to thank the National Science Council of the Republic of China, Taiwan for financially supporting (NSC98-2320-B-019-001-MY3). Ted Knoy is appreciated for his editorial assistance.

References

[1] E.O. Elvevoll, D. James, The emerging importance of dietary lipids, quantity and quality, in the global disease burden: the potential of aquatic resources, Nutr. Health 15 (3–4) (2001) 155–167.
[2] E.O Elvevoll, B. Osterud, Impact of processing on nutritional quality of marine food items, Forum Nutr. 56 (2003) 337–340.
[3] M. Holá, J. Kalvoda, H. Nováková, R. Skoda, V. Kanicky, Possibilities of LA-ICP-MS technique for the spatial elemental analysis of the recent fish scales: line scan vs. depth profiling, Appl. Surf. Sci. 257 (6) (2011) 1932–1940.
[4] C.C. Lin, R. Ritch, S.M. Lin, M.H. Ni, Y.C. Chang, Y.L. Lu, H.J. Lai, F.H. Lin, A new fish scale-derived scaffold for corneal regeneration, Eur. Cell. Mater. 19 (2010) 50–57.
[5] F. Pati, B. Adhikari, S. Dhara, Isolation and characterization of fish scale collagen of higher thermal stability, Bioresour. Technol. 101 (10) (2010) 3737–3742.
[6] C. Solomons, Protein in fish scale, S. Afr. J. Med. Sci. 20 (1) (1955) 27–28.
[7] H.J. Chai, J.H. Li, H.N. Huang, T.L. Li, Y.L. Chan, C.Y. Shiau, C.J. Wu, Effects of sizes and conformations of fish-scale collagen peptides on facial skin qualities and transdermal penetration efficiency, J. Biomed. Biotechnol. 2010 (2010) 757301.
[8] S. Chen, N. Hirota, M. Okuda, M. Takeguchi, H. Kobayashi, N. Hanagata, T. Ikoma, Microstructures and rheological properties of tilapia fish-scale collagen hydrogels with aligned fibrils fabricated under magnetic fields, Acta Biomater. (2010).
[9] M. Okuda, M. Takeguchi, M. Tagaya, T. Tonegawa, A. Hashimoto, N. Hanagata, T. Ikoma, Elemental distribution analysis of type I collagen fibrils in tilapia fish scale with energy-filtered transmission electron microscope, Micron 40 (5–6) (2009) 665–668.
[10] S. Itoh, M. Kikuchi, K. Takakuda, Y. Koyama, H.N. Matsumoto, S. Ichinose, J. Tanaka, T. Kawauchi, K. Shinomiya, The biocompatibility and osteoconductive activity of a novel hydroxyapatite/collagen composite biomaterial, and its function as a carrier of rhBMP-2, J. Biomed. Mater. Res. 54 (3) (2001) 445–453.
[11] M.B Nair, H.K. Varma, K.V. Menon, S.J. Shenoy, A. John, Reconstruction of goat femur segmental defects using triphasic ceramic-coated hydroxyapatite in combination with autologous cells and platelet-rich plasma, Acta Biomater. 5 (5) (2009) 1742–1755.
[12] K.P. Sanosh, M.C. Chu, A. Balakrishnan, T.N. Kim, S.J. Cho, Utilization of biowaste eggshells to synthesize nanocrystalline hydroxyapatite powders, Mater. Lett. 63 (2009) 2100–2102.
[13] N.A.M. Barakat, M.S. Khil, A.M. Omran, F.A. Sheikh, H.Y. Kim, Extraction of pure natural hydroxyapatite from the bovine bones bio waste by three different methods, J. Mater. Process. Technol. 209 (2009) 3408–4315.
[14] W. Cui, X. Li, S. Zhou, J. Weng, In situ growth of hydroxyapatite within electrospun poly(DL-lactide) fibers, J. Biomed. Mater. Res. A 82 (4) (2007) 831–841.

[15] T. Mygind, M. Stiehler, A. Baatrup, H. Li, X. Zou, A. Flyvbjerg, M. Kassem, C. Bunger, Mesenchymal stem cell ingrowth and differentiation on coralline hydroxyapatite scaffolds, Biomaterials 28 (6) (2007) 1036–1047.
[16] J.H. Rocha, A.F. Lemos, S. Agathopoulos, P. Valerio, S. Kannan, F.N. Oktar, J.M. Ferreira, Scaffolds for bone restoration from cuttlefish, Bone 37 (6) (2005) 850–857.
[17] S. Sarig, F. Kahana, Rapid formation of nanocrystalline apatite, J. Cryst. Growth 237 (2002) 55–59.
[18] Y.X. Pang, X. Bao, Influence of temperature, ripening time and calcination on the morphology and crystallinity of hydroxyapatite nanoparticles, J. Eur. Ceram. Soc. 23 (10) (2003) 1697–1704.
[19] J.L Xu, K.A. Khor, Z.L. Dong, Y.W. Gu, R. Kumar, P. Cheang, Preparation and characterization of nano-sized hydroxyapatite powders produced in a radio frequency (rf) thermal plasma, Mater. Sci. Eng.: A-Struct. 374 (1–2) (2004) 101–108.
[20] M.B. Jacobs, Micro-Kjeldahl method for biologicals, J. Am. Pharm. Assoc. Am. Pharm. Assoc. 40 (3) (1951) 151–153.
[21] K. Miyajima, Effects of periodic tension on osteoblast-like cells for cell differentiation and alkaline phosphatase activity, Nippon Kyosei Shika Gakkai Zasshi 49 (3) (1990) 226–236.
[22] J. Trommershauser, P.W. Glimcher, K.R. Gegenfurtner, Visual processing, learning and feedback in the primate eye movement system, Trends Neurosci. 32 (11) (2009) 583–590.
[23] M Motskin, D.M. Wright, K. Muller, N. Kyle, T.G. Gard, A.E. Porter, J.N. Skepper, Hydroxyapatite nano and microparticles: correlation of particle properties with cytotoxicity and biostability, Biomaterials 30 (19) (2009) 3307–3317.
[24] Y. Yuan, C. Liu, J. Qian, J. Wang, Y. Zhang, Size-mediated cytotoxicity and apoptosis of hydroxyapatite nanoparticles in human hepatoma HepG2 cells, Biomaterials 31 (4) (2010) 730–740.
[25] S. Pezzatini, R. Solito, L. Morbidelli, S. Lamponi, E. Boanini, A. Bigi, M. Ziche, The effect of hydroxyapatite nanocrystals on microvascular endothelial cell viability and functions, J. Biomed. Mater. Res. A 76 (3) (2006) 656–663.
[26] J. Scheel, S. Weimans, A. Thiemann, E. Heisler, M. Hermann, Exposure of the murine RAW 264.7 macrophage cell line to hydroxyapatite dispersions of various composition and morphology: assessment of cytotoxicity, activation and stress response, Toxicol. In Vitro 23 (3) (2009) 531–538.
[27] M. Lampin, C. Warocquier, C. Legris, M. Degrange, M.F. Sigot-Luizard, Correlation between substratum roughness and wettability, cell adhesion, and cell migration, J. Biomed. Mater. Res. 36 (1) (1997) 99–108.
[28] D.D Deligianni, N.D. Katsala, P.G. Koutsoukos, Y.F. Missirlis, Effect of surface roughness of hydroxyapatite on human bone marrow cell adhesion, proliferation, differentiation and detachment strength, Biomaterials 22 (1) (2001) 87–96.
[29] M. Lee, J. Hodler, P. Haghighi, D. Resnick, Bone excrescence at the medial base of the distal phalanx of the first toe: normal variant, reactive change, or neoplasia? Skelet. Radiol. 21 (3) (1992) 161–165.
[30] J.E Aubin, Bone stem cells, J. Cell. Biochem. Suppl. 30–31 (1998) 73–82.
[31] N. Fratzl-Zelman, P. Fratzl, H. Horandner, B. Grabner, F. Varga, A. Ellinger, K. Klaushofer, Matrix mineralization in MC3T3-E1 cell cultures initiated by beta-glycerophosphate pulse, Bone 23 (6) (1998) 511–520.